IPG 2023
INTERNATIONAL PIPELINE GEOTECHNICAL CONFERENCE
23 y 24 de Noviembre
Bogotá Plaza Hotel. Bogotá D.C. - Colombia
Con el auspicio de: arpel
Organiza: C-IPG ACIEM Asociación Colombiana de Ingenieros
6ª CONFERENCIA INTERNACIONAL GEOTECNIA DE DUCTOS
IPG2023-0023

ENVIRONMENTAL MONITORING AND PIPELINE EROSION DETECTION

Fabien Ravet[1], Cristian Silva[2], Jorge Muguruza[2], Alexandre Goy[3], Etienne Rochat[3], Yvan Jacquat[1]

[1] Gradesens, Fribourg, Switzerland
[2] Hunt LNG Operating Company, Lima, Peru
[3] Omnisens, Morges, Switzerland

ABSTRACT

Distributed Temperature Sensing (DTS) has been widely used for infrastructure monitoring. Most common applications are pipeline leak detection prevention and geohazard detection as well as power cable thermal rating. The study of the soil-atmosphere thermal interaction reveals that natural phenomenon can be monitored with DTS and buried communication Optical Fiber Cables (OFC). The current article discusses the application of DTS to the monitoring of the effect of soil-atmosphere thermal interaction showing annual and daily variations. DTS data from over 10 years is analyzed, allowing for the observation of the El Niño 2014-2016 event, which is among the strongest of the recent El Niño Southern Oscillation (ENSO) occurrences. It illustrates how DTS technology and communication backbone can provide data to study environmental effects at a global level. In addition, erosion can be monitored using DTS based system. Erosion is a natural hazard that threatens transportation infrastructures, and more specifically leads to pipeline exposure. The advantage of DTS is not only the erosion detection but also its localization with meter accuracy. A correlation analysis is introduced to quantify erosion by estimating the Depth-of-Cover (DoC). DoC can also be spatially profiled. Erosion events are detected and compared with periodic surveys.

Keywords: Distributed Temperature Sensing (DTS); Erosion; Depth-of-Cover; Environmental Monitoring; El Niño; Geohazards; Soil-Atmosphere Thermal Interaction

NOMENCLATURE

DoC or/and z_0 – Depth of Cover
DOFS – Distributed Optical Fiber Sensor
DTS – Distributed Temperature Sensing
DTSS – Distributed Temperature and Strain Sensing
ENSO - El Niño Southern Oscillation
OFC –Optical Fiber Cable
ONI - Oceanic Niño Index
SMC – Strain Monitoring Cable
TMC – Temperature Monitoring Cable

1. INTRODUCTION

Transportation infrastructures such as highways, railways or pipelines are commonly using optical fiber cable (OFC) for their communication and control systems. Often, the spare fibers commonly known as dark fibers are leased to telecommunication operators to develop their backbone. Some fibers are used by the transportation infrastructure owner or operator to monitor the integrity of their assets with Distributed Optical Fiber Sensing (DOFS). The purpose of such monitoring is to prevent failures and service interruption caused by human activities and natural hazards or to perform environmental monitoring ([1], [2]). A comprehensive introduction to DOFS is available in references [2] and [3]. Among the various techniques being used for infrastructure monitoring, Distributed Temperature Sensing (DTS) is an approach usually implemented for leak detection in hydrocarbon transport system or power cable temperature rating.

The present work introduces how DTS data analysis can also be used to localize events caused by hydraulic and aeolian erosion as well as to quantify the Depth-of-Cover (DoC) as discussed in references [4], [5] and [6]. As the DoC estimation relies on the understanding of the soil thermal response to environmental changes in combination with DTS data, the analysis can also lead to the monitoring of environmental changes and of the climate. Such application is also introduced in this article and is illustrated by the observation of the El Niño event (event 2014-2016).

2. THE PERU LNG PIPELINE

The PERU LNG transport system is composed of a 34" diameter high pressure pipeline operated by Hunt LOC. The pipeline is connected to the Transportadora de Gas del Perú

(TGP) pipeline in Chiquintirca. It spans over 408 km through the Andes down to the Peruvian coast after reaching a record-breaking altitude of 4901 m ([7], [8], [9]). The pipeline crosses about 300 km of challenging mountain terrain and 100 km of a coastal desert plain. Both Natural Gas (NG) transport system routes are presented in FIGURE 1.

FIGURE 1: PERU LNG (BLUE) AND TGP (RED) PIPELINE ROUTES.

From Chiquintirca to Ayacucho, the pipeline passes through the so-called "Sierra" region (FIGURE 2) where it is exposed to a high risk of landslides[7]. That specific part of the route, between the Meter Station in Chiquintirca and the second Main Line Valve (MLV-02) in Ayacucho, was instrumented since the construction with a permanent Geotechnical Monitoring System (GTMS) based on optical fiber sensing technology [8]. It has been in operation since June 2010.

FIGURE 2: PIPELINE ROW NEAR CHIQUINTIRCA, SIERRA REGION

Landslides are not the only geohazards to which the pipeline is exposed. In the Sierra section of the pipeline, erosion of hydraulic origin is the natural hazard that must be accounted for. In the coastal section, the pipeline route goes through sand dunes (FIGURE 3). The sand dune area is localized between MLV-10 and MLV-12 in Pisco Department. These dunes move under the effect of wind resulting in the so called eolian erosion which reduces the pipeline cover and eventually leaves it exposed (FIGURE 4). As presented in reference [10], periodic surveys require walking along the ROW to control sand markers. The approach is implemented to control the sand cover and eventually take corrective measures. Sand markers as well as metal detectors help determining the DoC during inspections. In 2019, a DTS interrogator has been installed in MLV11 to take advantage of the FOC running aside the pipeline and take advantage of its sensitivity to temperature as well as its ability to detect erosion [4].

FIGURE 3: TYPICAL LANDSCAPE OF THE PERU LNG PIPELINE IN THE SAND DUNE REGION.

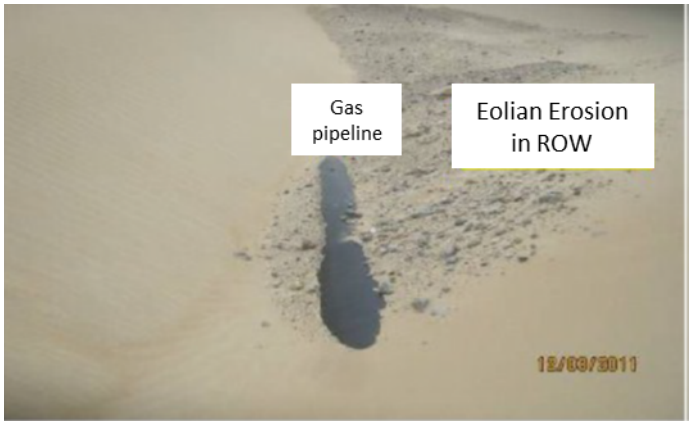

FIGURE 4: OBSERVATION IN JUNE 2011 OF PIPELINE EXPOSURE IN KP328+685 DUE TO EOLIAN EROSION ([10], [4]).

3. SENSING TECHNOLOGY AND MONITORING SYSTEM

1.1 Geotechnical Monitoring System

The implemented GTMS operational since 2010 in the Sierra section is composed of the following components:

- One DTSS, model DITEST TL, installed in MLV-01 since August 2019 measuring the first 60km of the pipeline between Chiquintirca and Ayacucho (FIGURE 5); the DITEST TL replaced the DITEST STA-R which in operation from June 2010 until August 2019
- SMC and TMC as strain and temperature measurement cable sensors;
- Monitoring software including measuring unit control, GIS (Geographical Information System) visualization and configuration as well as possible connection to the SCADA.

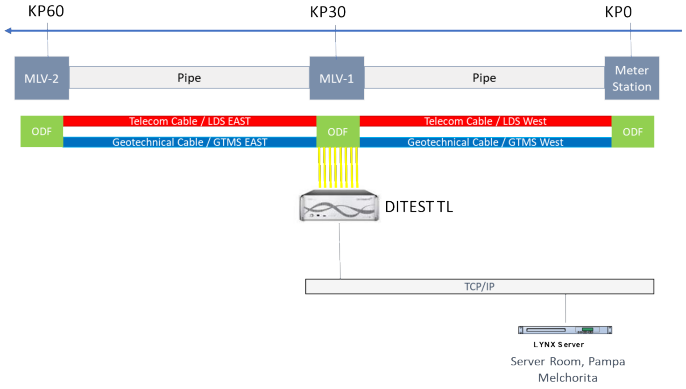

FIGURE 5: MONITORING ARCHITECTURE IMPLEMENTED IN THE SIERRA SECTION.

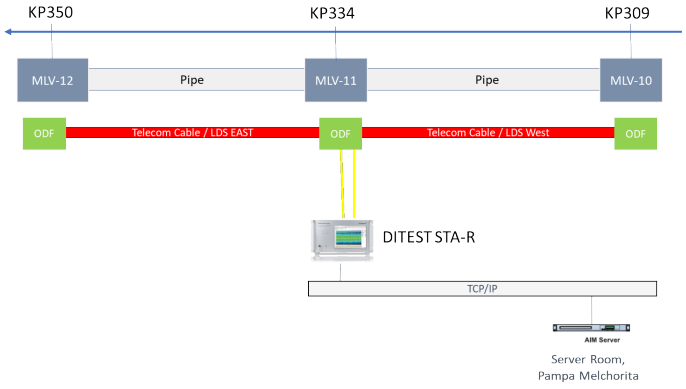

FIGURE 6: MONITORING ARCHITECTURE IMPLEMENTED IN THE DUNE SECTION.

Specific details about the GTMS installation and use in the Peru LNG pipeline project is presented in [8]. Other examples of real-world implementations along pipelines and transportation infrastructures can be found in references [1] and [2].

In August 2019, the DITEST STA-R was moved from MLV-01 to MLV-11, near Pisco, covering 41km of the pipeline to expand the monitoring to the dune section of the transport system. Monitoring architecture is presented in FIGURE 6. Only the telecom cable is used as a temperature sensor.

1.2 Measurement Principle of the Interrogators

The core instrumentation of the GTMS relies on Brillouin Optical Time Domain Analyzer or (BOTDA) or Brillouin optical Time Domain Reflectometer (BOTDR) interrogators. BOTDA uses stimulated Brillouin scattering (SBS) in single-mode fiber. Brillouin scattered light is characterized by a frequency shift proportional to both temperature and strain variations. This shift can be measured by analyzing the interaction in standard optical fibers between a pump lightwave (pulse) and a counter-propagating probe lightwave (continuous). Such interrogator can use a broad variety of SMF such as the ITU G.652 or G.657. Typically, the Brillouin frequency shift at ambient temperature of such fiber ranges from 10.7 to 11.0 GHz at 1.55 □m wavelength and varies with strain and temperature coefficients of 0.05 MHz□ε and 1 MHz/°C respectively. This linear relationship makes it an easy method for sensing mechanical and thermal effects, whilst the pulse nature of the pump lightwave allows for accurate localization (time of flight measurement) and defines spatial resolution (pulse duration). The discrimination of strain from temperature measurement is easily completed by using two distinct sensing cables. Telecommunication cables are generally good temperature sensors as the fibers are isolated mechanically (loose tube design). Strain sensing is achieved with dedicated cable (tight buffered design) in which thermal effects must be compensated by temperature measurements from a telecommunication cable. Detailed reviews and general introduction about distributed sensing technology are presented in references [2] and [3].

Further details on the measuring unit configuration, fiber sensitivity to strain and temperature as well as sensing parameter definitions can be found in Niklès works ([11], [12], [13]). Measurement distance range of about 80 km per sensor can be achieved. Longer range has been demonstrated thanks to the use of in-line optical amplification [14]. Performance parameter definitions and verification testing are now formalized in the IEC 61757-3-1 standard for DTS application. The same IEC committee is currently working on a DSS standard. The definitions of the most common parameters are presented in Appendix 1.

1.3 Sensing and Communication Cables

Temperature Measurement Cables (TMC) are high quality grade versions of standard armored telecommunication fiber optics cable usually used for direct burial applications. The cable includes the SMF used for temperature monitoring as well as fibers for data communication between the instruments and the control room. The cable used in this project has a triple-jacket, double-armored structure. Such design aims at strengthening the cable for direct burial use in challenging environments. Further mechanical isolation is guaranteed by the loose tube design with large excess fiber length.

As a general comment, it is key that mechanical and optical characteristics of all sensing and communication cables comply with IEC 794-1 Optical Fiber Cables Specification.

4. GEOHAZARDS AND SENSING METHOD

The GTMS aims at detecting and locating at an early stage all the natural events that can be a threat to the pipeline. It will emphasize the early signs of these threats. Geohazards and associated sensing quantities which are either strain or temperature are listed in TABLE 1 from reference [1].

TABLE 1. GEOHAZARDS AND SENSING METHODS.

Geohazard	Soil Strain Measurement	Soil Temperature Measurement
Erosion		X
Landslide [15]	X	
Subsidence	X	

The following subsections bring the theoretical background sustaining the use of the temperature sensing component of the GTMS to detect geohazards associated with erosion.

5. SOIL-ATMOSPHERE INTERACTION

In References [1], [2] , [4], [5] and [6], we discussed the use of DTS for natural hazard monitoring. In these works, temperature spatial and temporal profiles characterizing erosion were evidenced and categorized. Other patterns experiencing periodic behaviors were observed. What was shown can be illustrated by a selection of behaviors presented in FIGURE 7. The figure displays three distinct positions over a three-month duration. The relative temperature at one position remains steady (6243m, green curve). A second position experiences a progressive increase (5047m, grey curve). The last position (6351m, red curve), which is a localized event, follows a similar thermal trend as point 5047m but presents oscillations. Zooming on a five-day duration and including the ambient temperature evolution on the same graph, we identify two features (FIGURE 8). First, the oscillations at position 6351m have a period of 24 hours. Second, the oscillations are shifted by 10 hours. These two features are directly related to the depth of burial of the temperature probe (e.g. the OFC measured with a DTS) in the soil. To understand these temperature profiles and discriminate information about possible threats from other causes, the soil-atmosphere interaction was studied based on reference [16].

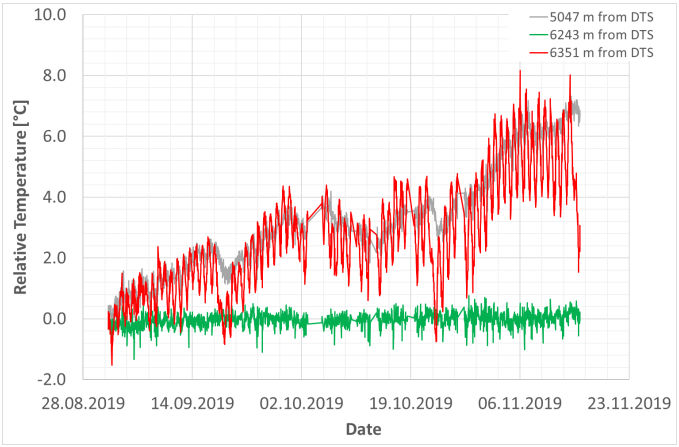

FIGURE 7: THREE MONTHS EVOLUTION OF THE RELATIVE TEMPERATURES OBTAINED FROM DTS MEASUREMENTS ON AN OFC LAID ALONG A PIPELINE ([4], [5]).

Fourier's work regarding heat propagation in solids, dating back to 1822, leads to the second law of heat conduction, also known as the equation of diffusion. Using Hillel assumptions, in particular that the heat source varies periodically at two paces, yearly and daily [16], and applying the resolution to the case of DTS monitoring along a natural gas pipeline in Peru ([4], [5]), one get the temperature dependence against time (t) and depth (z)

$$T(z,t) = \bar{T} + T_y(z,t) + T_d(z,t) = \bar{T} + A_y(0)\,sin(\omega_y t - z/d_y)e^{-z/d_y} + A_d(0)\,sin(\omega_d t - z/d_d)e^{-z/d_d}$$

where $\bar{T}$ is the annual average, $T_y(z,t)$ is the annual temperature, $T_d(z,t)$ is the diurnal temperature, while $A_y(0)$ and $A_d(0)$ are the surface annual and diurnal amplitudes respectively. The temporal behaviour is controlled by the annual and diurnal radial frequencies noted ω_y and ω_d respectively. Two parameters are introduced, which are the annual and diurnal damping depths, noted d_y and d_d respectively and defined as $d_y = \sqrt{2\,D/\omega_y}$, and, $d_d = \sqrt{2\,D/\omega_d}$. D is the thermal diffusivity coefficient, which is defined as the ratio of the thermal conductivity κ to the volumetric heat capacity C_v. D depends on soil chemical

composition, water content, grain size and porosity. The form of these equations assumes that D is independent on depth which is a reasonable assumption as the OFC are usually buried in a trench presenting uniform soil conditions.

6. EROSION MONITORING AND DOC QUANTIFICATION

The developed thermal model not only confirms that the periodic behaviour observed in DTS data can be used to identify the occurrence of erosion, but it also allows for the quantification of the severity of the hazard by analysing the time lag in the daily temperature measurements to estimate the *DoC*. By measuring the temperature temporal evolution on the surface and at the depth of interest z_0, we can then calculate the phase difference between the two depths. The resolution leads to the following formula:

$$DoC \equiv z_0 = \tau\sqrt{2D\omega_d} = \sqrt{\frac{2D}{\omega_d}}\, ln\left[\frac{\bar{T}-T(z,t'_{max})}{\bar{T}-T(0,t''_{max})\bar{T}}\right] \quad (1)$$

where τ is the measured time lag between the maximum temperature at the surface and at z_0. A similar formula can be obtained by calculating the ratio between the maximum amplitude at the surface and at z_0. In that formula, t'_{max} and t''_{max} are the time at the maximum amplitude at depth z and the surface, respectively.

Real data are not perfect sinusoids due to measurement noise and other heat sources. To improve the robustness of the approach, we introduce a direct processing of the raw data without any consideration regarding the existence of an event. First, we remember that the ambient temperature stimulus is periodic. Second, we know that the soil response is such that there must be a similar but delayed behavior. We then compute the correlation between the ambient temperature (stimulus) measured in a nearby meteorological station $T_{weather}(t)$ and the temperature measured with DTS $T_{DTS}(x,t)$ (response) at the OFC depth where x is the position along the fiber and t is the measurement time-stamp. The correlation must be computed at every position x of the OFC, i.e. regardless of evidence of events, over a temporal sample size of minimum $2\pi/\omega_d$ as

$$X(x,\tau) = \frac{\omega_d}{2\pi}\int_0^{2\pi/\omega_d} T_{weather}(t+\tau)T_{DTS}(x,t)dt \quad (2)$$

Then solving (3) for $T_{weather}(t)=T_d(0,t)$ and $T_{DTS}(z,t)=T_d(z,t)$, the maximization of the $X(\tau)$ leads to relations (2). For raw data, relation (2), its left member remains the same while its right member must be expressed as

$$DoC(x) \equiv z_0(x) = \sqrt{\frac{2D}{\omega_d}}\, ln\left[\frac{1}{2}\frac{T^2_{weather,max}}{X_{max}(x)}\right] \quad (3)$$

where $T_{weather,max}$ is the maximum of the autocorrelation of $T_{weather}(t)$ and $X_{max}(x)$ is the maximum of $X(x,\tau)$.

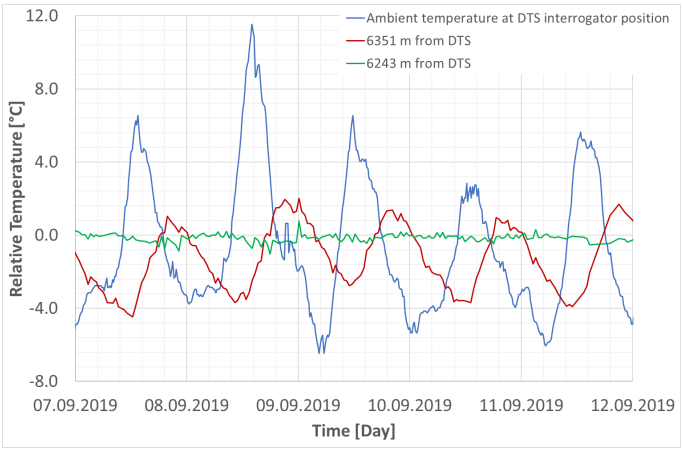

FIGURE 8: FIVE DAYS EVOLUTION OF THE RELATIVE TEMPERATURES OBTAINED FROM DTS MEASUREMENTS ON AN OFC LAID ALONG A PIPELINE ([4], [5])

In August 2019, a pilot project has been initiated to monitor sand dune migration and eolian erosion along a pipeline buried in the coastal desert of Peru [4]. Within that context, a total of 41km was monitored with a Brillouin Optical Time Domain Analyzer, (BOTDA) whose spatial resolution is 2m and its temperature repeatability (σ) is better than 0.5°C. Temporal evolutions presented in FIGURE 7 and FIGURE 8 as well as the profiles of FIGURE 9 are characteristic examples of what has been measured during the 3-months pilot project.

FIGURE 9 displays the temperature profiles zoomed on a section of 300m. It shows three events whose amplitudes vary with a period of 24 hours. Event 1 temporal evolution is presented in Figure 2 (at 6351m). The two other events have similar temporal evolution with lower amplitude. Event 1 also features a time lag relative to the ambient temperature.

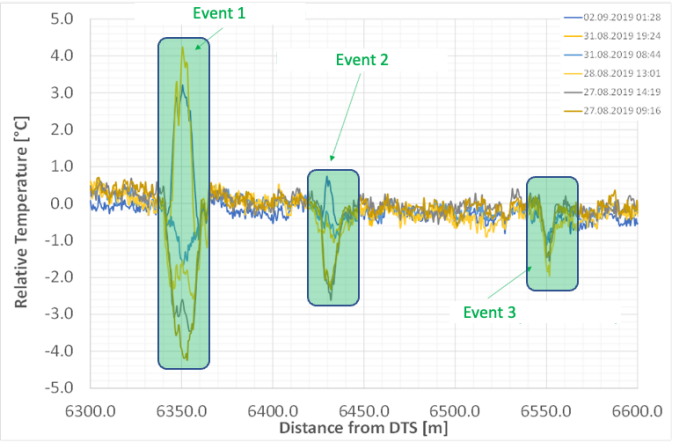

FIGURE 9: TEMPERATURE PROFILES CAPTURED DURING ONE WEEK AND ZOOMED ON A SECTION 300M LONG [16].

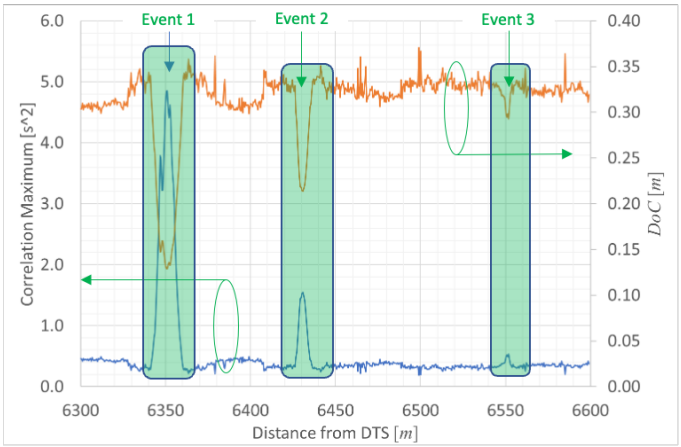

FIGURE 10: X_{max} AND *DoC* PROFILES COMPUTED WITH *D* FOR DRY SAND ($0.2x10^{-6}$ m^2/s) FROM DATA OF REFERENCE [16].

In the present work, we apply the correlation analysis to a subset of the data composed of profiles measured every 15 minutes from August 27th to November 15th, 2019. The data subset must have a length of at least 24 hours. FIGURE 10 displays the result of the correlation computation using relation (4), as well as the DoC profile obtained from relation (2) and sinusoidal curve fitting [4]. Only the section of interest, between 6300m and 6600m is discussed, as no other event of importance appeared along the rest of the sensor during the whole pilot duration. The smallest DoC per event is reported in last row of TABLE 2. A discrepancy of maximum 5 cm is observed between correlation analysis and curve fitting approach.

According to Difference is higher for Event 3. Deviation increases from event 1, which is closer to the surface, to event 3. As the temperature measurement repeatability is 0.5°C, deeper event must be more difficult to detect. In fact, the amplitude of the temperature variation reduces with depth ([1], [4]). Therefore, it influences the DoC estimation with a larger uncertainty as the measurement noise increases. The influence of the measurement repeatability on the DoC estimation uncertainty should be studied for both approaches and compared.

TABLE 2. Event analysis using *D* of dry sand [16].

	Event 1	**Event 2**	**Event 3**
DTS Distance	6350 m	6431 m	6551 m
Event Length	20 m	11 m	5 m
DoC [4]	0.14 cm	0.25 cm	0.34 cm
DoC [5]	0.13 cm	0.21 cm	0.29 cm

Site survey has confirmed the three events along the pipeline ROW between 6300m and 6600m. No additional events were found during the survey. The site survey method indicates that these events present a DoC comprised between 50 cm and 80 cm [10] while we find that it varies from 10 to 30 cm. The site survey DoC values are larger than the DoC estimated with the DTS. The difference comes from the position of the cable relative to the pipeline. By construction during this project, the cable was laid at a depth that is at best at the same level as the top of the pipeline and 3 m left or right from the pipeline central axis. Over time, the cable relative position could have varied as soil usually settles around the pipe. That effect can be compensated in new constructions by purposely designing the cable installation method. Another cause for the difference can be the variability of the value of D which depends on grain size and porosity for a given composition and water content. At this stage of the study, these parameters are not available. This is probably the ultimate limitation of this approach.

7. EL NIÑO EPISODE

A long-term monitoring can also reveal other interesting features. FIGURE 11 displays the temperature evolution measured at a distance of 1469 m from a DTS between June 2010 and December 2019, near the town of San Miguel (La Mar Province, Ayacucho Department) in the Sierra region of the Peruvian Andes ([4], [6]). A 365 days periodic signal is observed, without any visible daily variations as shown by the blue (raw data) curve. An additional feature must be noted. The measured temperature presents a trend which increases with a peak value comprised between 15.12.2014 and 15.01.2016, and then followed by a progressive decrease.

Comparing these measurements with long term meteorological data suggest that the observed pattern can be related to one phase of El Niño Southern Oscillation (ENSO). ENSO is a variation of the Southeastern Pacific Ocean surface temperature and is characterized by the Oceanic Niño Index (ONI) [17]. In fact, a strong occurrence has been reported and is known as El Niño 2014-2016 warm episode as shown in Figure 5 by the ONI. It usually strongly influences the climate of South America Pacific coast and can cause severe droughts.

Despite the difficulty of modelling El Niño due to its extreme variability and to the complexity of the phenomenon that are at stake, we considered a model that is a linear combination of two sinusoids, one with a 365 days period and the other with a period of 7 years. El Niño oscillation has a period that is comprised between 2 to 7 years [18]. In addition to temperature raw data (blue curve), FIGURE 11 displays the fit of the oscillations of the annual change (red curve) and the El Niño trending (grey curve).

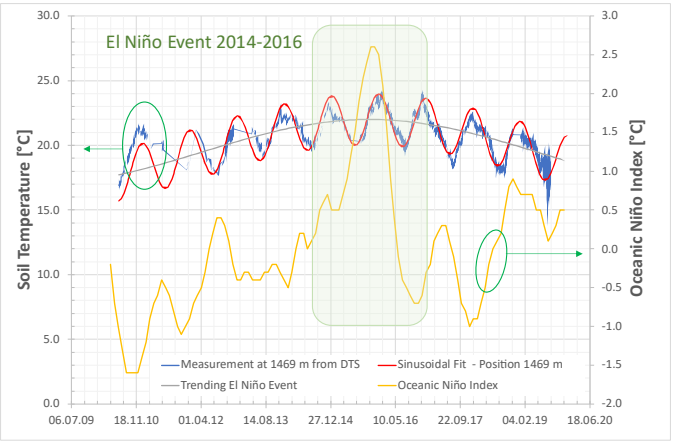

FIGURE 11: MONTHLY TEMPERATURE EVOLUTION FROM 2010 TO 2019 (DTS DATA, SINUSOIDAL FITTING) AND ONI [6].

8. CONCLUSIONS

Large transportation infrastructures equipped with communication OFC can be protected by permanent monitoring using DOFS. The analysis of DTS data can detect and localize erosion. It also shows that the erosion can be quantified helping the infrastructure owner to take mitigation measures in a timely manner. The permanent monitoring can also provide data for environmental long-term surveys. Such application goes beyond soil-atmosphere thermal interaction and can also be implemented with submarine cables. The combination of temperature data captured from terrestrial and subsea networks will contribute to the improvement of the understanding of global soil, water and atmosphere interactions.

ACKNOWLEDGMENT

The authors would like to acknowledge Omnisens and Gradesens teams for the continuous support. Furthermore, the authors are grateful to Hunt LOC/Peru LNG for the long-lasting fruitful cooperation and appreciated feedbacks.

REFERENCES

[1] Ravet, F., Briffod, F., Goy, A. *et al.* "Mitigation of geohazard risk along transportation infrastructures with optical fiber distributed sensing". *J Civil Struct Health Monit* **11**, 967–988 (2021). https://doi.org/10.1007/s13349-021-00492-x

[2] Ip, E., Ravet, F., Martins, H. *et al.,* "Using Global Existing Fiber Networks for Environmental Sensing" in Proceedings of the IEEE, vol. 110, no. 11, pp. 1853-1888, Nov. 2022, https://doi.org/10.1109/JPROC.2022.3199742.

[3] Hartog, A.H. (2017). "An Introduction to Distributed Optical Fibre Sensors (1st ed.)". CRC Press. https://doi.org/10.1201/9781315119014

[4] Ravet, F., Silva, C., Gil, R. *et al.* "Distributed Temperature Sensing for Erosion Detection and DoC Estimation: The Peru LNG Experience in Ayacucho and Ica Departments." *Proc. of the ASME-ARPEL 2021 International Pipeline Geotechnical Conference.* https://doi.org/10.1115/IPG2021-64159

[5] Ravet F., Goy, A., Rochat, E. "Distributed Temperature Sensing Data Analysis to Prevent Erosion and Estimate Depth-of-Cover," in 27th International Conference on Optical Fiber Sensors, Technical Digest Series (Optica Publishing Group, 2022), paper W4.7. https://doi.org/10.1364/OFS.2022.W4.7.

[6] Ravet, F., Silva, C., Muguruza, J., *et al.* "Correlation of El Niño 2014-2016 Episode with DTS Data". in Proceedings of the SPIE, Euorpean Workshop on Optical Fiber Sensors, EWOFS 2023.

[7] Gasca, A., Gutierrez, E., "The Challenge of Crossing the Andes: A Data Base Analysis and Peru LNG Project Description", 1st International Pipeline Geotechnical Conference, Bogotá, Colombia, Paper IPG2013-1951 (2013). https://doi.org/10.1115/IPG2013-1951

[8] Ravet, F., Ortiz, E.G., Peterson, B., Hoglund, G. andNiklès, M. (2011). "Geohazard prevention with online continuous fiber optic monitoring." Proc. of the Rio Pipeline Conference and Exposition, Rio de Janeiro, Brazil, Paper IBP1277_11 (2011).

[9] Pipeline International, March 2011. "A long and winding route: overcoming terrain challenges on the Peru LNG pipeline", pp.27-29

[10] Silva, C., "Sand Markers – Peru LNG Pipeline", 2nd International Pipeline Geotechnical Conference, Bogotá, Colombia, Paper IPG2015-1924 (2015)

[11] Niklès, M., Thévenaz, L., Robert PH. (1996). "Simple distributed fiber sensor based on Brillouin gain spectrum analysis." Optics Letter 21(10), pp.758-760. https://doi.org/10.1364/OL.21.000758

[12] Niklès, M., Thévenaz, L., Robert PH. (1997). "Brillouin gain spectrum characterization in single-mode optical fibers." Journal of Lightwave Technology, JLT-15, pp. 1842-1851. https://doi.org/10.1109/50.633570

[13] Niklès, M. (2007). "Fibre optic distributed scattering sensing system: perspectives and challenges for high performance applications." 3rd European Workshop on Optical Fibre Sensors, A. Cutolo, B. Culshaw, J. M. Lopez-Higuera eds., Proc. of SPIE Vol. 6619, 66190D. https://doi.org/10.1117/12.738349

[14] Gyger, F., Chin, S., Rochat, E., Niklès, M., Ravet, F., "Ultra Long Range DTS (>300km) to Support Deep Offshore and Long Tieback Developments" 33rd International Conference on Ocean, Offshore and Arctic Engineering, OMAE 2014, San Francisco, PAPER OMAE2014-24019. https://doi.org/10.1115/OMAE2014-24019

[15] Highland, L.M., and Bobrowsky, Peter, 2008, Highland, L.M., and Bobrowsky, Peter, 2008, The landslide handbook – A guide to understanding landslides:" Reston, Virginia, U.S. Geological Survey Circular 1325, 129p.

[16] Hillel, D. "Introduction to Soil Physics", Academic Press, 1972. https://doi.org/10.1016/B978-0-08-091869-3.50002-0.

[17] National Oceanic and Atmospheric Administration, https://www.climate.gov/news-features/understanding-climate/el-niño-and-la-niña-alert-system

[18] Climate Prediction Center (19 December 2005). "ENSO FAQ: How often do El Niño and La Niña typically occur?". National Centers for Environmental Prediction. Archived from the original on 27 August 2009. Retrieved 26 July 2009.

APPENDIX 1: Performance Parameter Definitions (as per IEC 61757-2-2)

Spatial Resolution

The spatial resolution is the ability to discriminate between two adjacent locations submitted to different temperature/ strain conditions. The spatial resolution is directly related to the optical pulse width, or the pulse length W illuminated by the pulse at a given time $w = \tau v_g/2$, where τ is the pulse width and v_g is the group velocity of the pulse. Spatial resolution also depends on receiver bandwidth.

Strain and Temperature Resolution – Measurement Repeatability

Strain and temperature resolutions are directly related to the measurement noise. The noise includes spontaneous, short duration deviations in output (reading) about the mean output (reading), which are not caused by temperature changes. The resolution is defined as twice the standard deviation of the noise (+/- twice the standard deviation includes 95.4% of the measurements).

Strain and Temperature Uncertainty

The Strain and temperature uncertainty is the difference between the measurement unit reading and the measurement obtained with a reference device. The measurement uncertainty depends on the calibration precision, i.e. on the quality of the calibration setup and procedure. For instance, the calibration of a piece of fiber as a temperature sensor requires a traceable reference temperature sensor with given uncertainty.

APPENDIX 2: GEOHAZARDS

Subsidence

Ground subsidence is the phenomenon described by a terrain surface moving downward relative to the surrounding soils. Subsidence can be caused by excessive ground water depletion, underground mining, limestone dissolution, natural gas extraction etc.

Landslide

Reference [15] gave a general definition of a landslide stating: "*A landslide is a downward sloping movement of rock, soil, or both, occurring in the rupture of a surface - rotational sliding or flat collapsing - in which most of the material moves as a coherent or semi-coherent mass, with small internal deformation*." The authors list and describe several type of landslides such as translational or rotational landslides as well as rock falls.

Erosion

Erosion is the phenomenon that removes soil or rock under the action of waterflow, wind or glaciers and transports the material to another location.